PRAMANA
— journal of
physics

Vol. 67, No. 6
December 2006
pp. 1155–1164

Photonic band gap engineering in 2D photonic crystals

YOGITA KALRA and R K SINHA
TIFAC-Center of Relevance & Excellence in Fiber Optics & Optical Communication, Department of Applied Physics, Delhi College of Engineering, Faculty of Technology (University of Delhi), Bawana Road, New Delhi 110 042, India
E-mail: yogita25@rediffmail.com; dr_rk_sinha@yahoo.com

MS received 5 January 2006; revised 16 July 2006; accepted 3 August 2006

Abstract. The polarization-dependent photonic band gaps (TM and TE polarizations) in two-dimensional photonic crystals with square lattices composed of air holes in dielectric and *vice versa* i.e., dielectric rods in air, using the plane-wave expansion method are investigated. We then study, how the photonic band gap size is affected by the changing ellipticity of the constituent air holes/dielectric rods. It is observed that the size of the photonic band gap changes with changing ellipticity of the constituent air holes/dielectric rods. Further, it is reported, how the photonic band gap size is affected by the change in the orientation of the constituent elliptical air holes/dielectric rods in 2D photonic crystals.

Keywords. Photonic crystal; photonic band gap; plane-wave expansion method.

PACS Nos 71.20; 42.70.Q

1. Introduction

Recently, photonic crystals (PhCs) have attracted much attention from both fundamental and practical viewpoints, due to their unique optical properties and their potential use in optical devices. These crystals have a periodic dielectric structure, with lattice spacing comparable to the wavelength of light [1,2]. The periodic dielectric structure affects the dispersion relations and spatial distribution of light traveling through the photonic crystal. There exist many analogies between the PhCs and the more familiar electronic crystals. In both cases, Brillouin zones that reflect the symmetry of the real space crystal can describe the reciprocal lattice. For large enough dielectric contrast, there exist wavelength regions where no solutions of Maxwell's equations in the periodic structure can be found, creating photonic band gaps. The existence of photonic band gap gives rise to a number of interesting and useful properties including the localization of light at defects and surfaces and the inhibition of radiation. Therefore, to take the maximal advantage of the ability

of photonic crystals to control electromagnetic radiation, study of photonic band gaps in photonic crystals is a must. The photonic band gaps in photonic crystals depend upon the arrangement of the constituent air holes/dielectric rods, fill factor and dielectric contrast of the two mediums used in forming photonic crystals. In the past, a lot of work has been reported on the design of 2D photonic crystals as well as their possible applications in the design of photonic band gap-based optical devices. Generally, in these studies 2D photonic crystals consist of arrays of circular holes/dielectric rods in dielectric/air in various lattice arrangements (square, triangular, etc.). It has been shown that with proper design of the shape of the constituent objects, the dielectric contrast between the host material and the constituent object material, lattice type, and filling factor (area/volume percentage occupied by the constituent objects), the position and size of photonic band gap (PBG) in a PhC can be engineered to meet the requirements of the specific applications [3–5]. However, in the recent past some studies on the photonic crystals consisting of elliptical air holes/dielectric columns have been done where the variation of complete photonic band gap with varying roundedness in a PhC consisting of air holes in a dielectric in a triangular lattice has been studied. Another study projects the method of obtaining complete photonic band gap with elliptical air holes in a dielectric medium in a rectangular lattice [6–9]. However, the complete photonic band gap can be obtained in few select structures, namely, triangular, honeycomb or rectangular lattice arrangements.

In this paper, we discuss the variation of photonic band gap size in both topologies of 2D PhCs, i.e. (i) PhC composed of dielectric rods in air and (ii) PhC composed of air holes in dielectric in square lattice because of the ellipticity of the constituent dielectric rods or air holes for transverse electric (TE) and transverse magnetic (TM) polarizations. We systematically study the effects of orientation of the dielectric rods/air holes in the respective cases and their shapes in square lattice. We demonstrate the optimization of the photonic band gap engineering through the introduction of asymmetry in the crystal lattice. The knowledge of the ellipticity-induced variation of the photonic band gap sizes in 2D PhCs in both the above-mentioned topologies can prove useful in the design of polarization-sensitive photonic band gap-based devices [10].

2. Design parameters of the PhCs

To analyze the variation of photonic band gap size with varying ellipticity, we considered the following two structures:

(i) PhC composed of square lattice of elliptical air holes in silicon (Si) ($n = 3.42$) as shown in figure 1a.

(ii) PhC composed of square lattice of elliptical silicon (Si) ($n = 3.42$) rods in air as shown in figure 1b.

Figure 1c depicts the model of the PhC consisting of square lattice of air holes in Si and figure 1d depicts the model of the PhC consisting of square lattice of elliptical Si rods in air. Figure 1e shows the Brillouin zone for the two structures used.

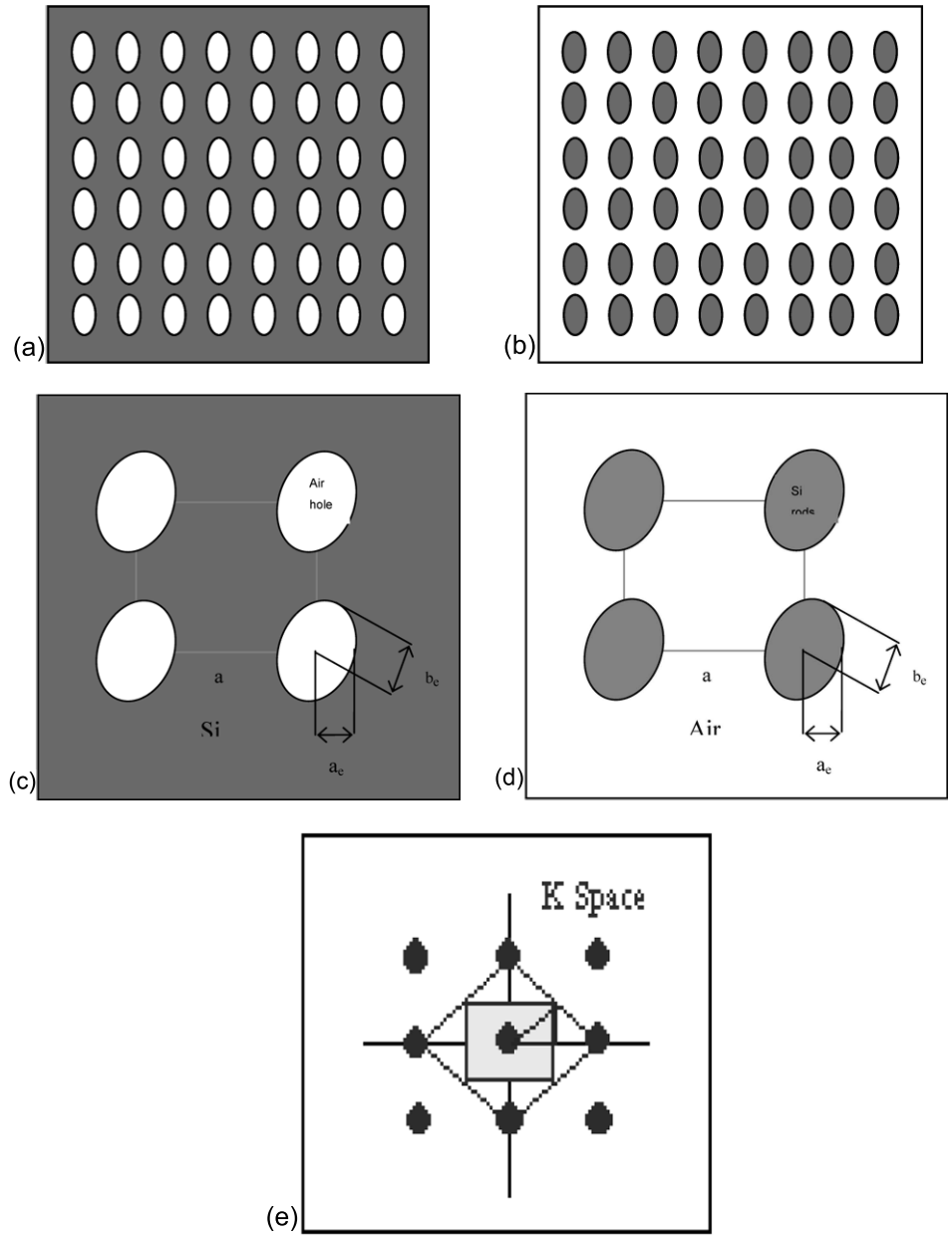

Figure 1. (**a**) PhC composed of a square lattice of elliptical air holes in Si. (**b**) PhC composed of square lattice of elliptical Si rods in air. (**c**) Model of the PhC composed of square lattice of elliptical air holes in Si. (**d**) Model of the PhC composed of square lattice of elliptical Si rods in air. (**e**) Brillouin zone of the square lattice of air holes/Si rods in Si/air.

The materials used to study the effect of ellipticity on the photonic band gap consist of silicon and air as they provide adequate dielectric contrast for obtaining photonic band gaps. Moreover, silicon is the most commonly used material in the design of various devices.

3. Numerical analysis and results

To obtain the photonic band diagrams of the considered photonic crystals, the plane-wave expansion (PWE) method has been employed, where both the electromagnetic field and the periodic dielectric structure are expanded in Fourier series [11]. For that the material has been assumed to be linear, locally isotropic and periodic with lattice vectors $\mathbf{R}$. The relative permeability μ is taken as 1 and the relative permittivity is defined as

$$\varepsilon(r) = \varepsilon_b + (\varepsilon_s - \varepsilon_b) f(r), \tag{1}$$

($f(r) = 1$ inside the column and =0 outside it) where ε_s is the dielectric constant of the columns and ε_s is the dielectric constant of the background respectively.

Because of two-dimensional lattice periodicity, the dielectric constant ε can be described as

$$\varepsilon(r) = \varepsilon(r + \mathbf{R}), \tag{2}$$

where vectors $\mathbf{R}$ are the vectors of the 2D lattice.

Solving Maxwell's equations for the magnetic field H_ω leads to the following vector wave equation:

$$\nabla \times \left(\frac{1}{\varepsilon(r)} \nabla \times H_\omega(r) \right) = \left(\frac{\omega}{c} \right)^2 H_\omega(r). \tag{3}$$

The magnetic field H_ω is then expanded into plane waves of wave vector $\mathbf{k}$ with respect to the 2D reciprocal lattice vectors $\mathbf{G}$

$$H_\omega(r) = \sum_{\mathbf{G}\lambda} h_{\mathbf{G}\lambda} \mathbf{e}_\lambda \mathrm{e}^{[i(\mathbf{k}+\mathbf{G})\mathbf{R}]}, \tag{4}$$

where the polarization vectors $\mathbf{e}_\lambda$ characterize two independent polarizations λ. Substituting eq. (4) in the vector wave eq. (3) provides an equation for the coefficients $h_{\mathbf{G}\lambda}$ given by

$$\sum_{\mathbf{G}'\lambda'} E^{\mathbf{k}}_{\mathbf{G}\lambda,\mathbf{G}'\lambda'} h_{\mathbf{G}'\lambda'} = \omega^2 h_{\mathbf{G}\lambda}. \tag{5}$$

The matrix E in the eigenvalue equation is defined as

$$E^{\mathbf{k}}_{\mathbf{G}\lambda,\mathbf{G}'\lambda'} = [(\mathbf{k}+\mathbf{G}) \times \mathbf{e}_\lambda] \, [(\mathbf{k}+\mathbf{G}') \times \mathbf{e}_{\lambda'}] \varepsilon^{-1}(\mathbf{G}, \mathbf{G}'). \tag{6}$$

The Fourier transform of the inverse dielectric constant

$$\varepsilon^{-1}(\mathbf{G}, \mathbf{G}') = \varepsilon^{-1}(\mathbf{G} - \mathbf{G}') \tag{7}$$

depends on the difference of the reciprocal lattice vectors only. The properties of $\varepsilon(r)$ are given by

$$\varepsilon^{-1}(\mathbf{G}) = \frac{1}{A}\int_A \varepsilon^{-1}(r)\mathrm{e}^{-i\mathbf{G}(r)}\mathrm{d}^2 r, \tag{8}$$

where A is the area of the unit cell.

By solving eq. (6) for 2D photonic crystals and in-plane propagation, the photonic band diagrams can be obtained for the two polarizations, namely, transverse electric (TE) polarization and transverse magnetic (TM) polarization.

3.1 *PhC composed of square lattice of air holes in Si*

First, the analysis has been done for the PhC structure composed of square lattice of air holes in Si. The variation of photonic band gaps in the case of elliptical holes/dielectric rods has been done under the following headings:

(i) Keeping the fill factor constant ($a_e b_e$ = constant).
(ii) Keeping the major axis b_e constant (ellipticity is induced by decreasing the minor axis).
(iii) Changing the orientation angle of the constituent air holes/dielectric rods.

Figure 2 shows the variation of TE1-2 photonic band gap size with the normalized air hole radius (r/a), which is the fictive radius of a circle having the same area as the ellipse considered, for three different ellipticities ($e = a_e/b_e$) of the constituent air holes, namely, $e = 1$, 0.95 and 0.9 keeping the fill factor constant. In this, the photonic band gap for TE polarization has been studied, as the photonic band gap does not exist for TM polarization.

From figure 2, it is evident that the TE1-2 photonic band gap first increases with the increase in normalized air hole radius r/a and then starts decreasing after a particular value for all the three cases. However, for a fixed value of r/a, the TE1-2 photonic band gap size decreases with the decreasing ellipticity. Figure 3 shows the variation of photonic band gap observed for $e = 1$, 0.95 and 0.9 for normalized fictive radius of air holes $r = 0.43a$ in Si.

From figure 3, it is evident that the photonic band gap size decreases with decreasing ellipticity of constituent air holes. Figure 4 shows the variation of TE1-2 photonic band gap size with the normalized major axis (b_e/a) for three different values of ellipticities, i.e. $e = 1$, 0.95 and 0.9, where major axis is kept constant and the ellipticity is induced by changing the minor axis. As decreasing the minor radius induces the ellipticity, this results in the decrease of the fill factor. Hence the graph shows the effect of both the ellipticity of air holes as well as the fill factor on the width of photonic band gaps. The photonic band gap size first increases with the increase in fill factor, becomes maximum for a particular b_e/a value and then starts decreasing for all three cases.

Then, the change in photonic band gap width with the change in the orientation angle of the constituent elliptical air holes has been studied for one particular value of r/a. Figure 5 shows the normalized photonic band gap size variation due to change in angle for $r = 0.43a$ keeping fill factor constant for $e = 1$, 0.95 and 0.9.

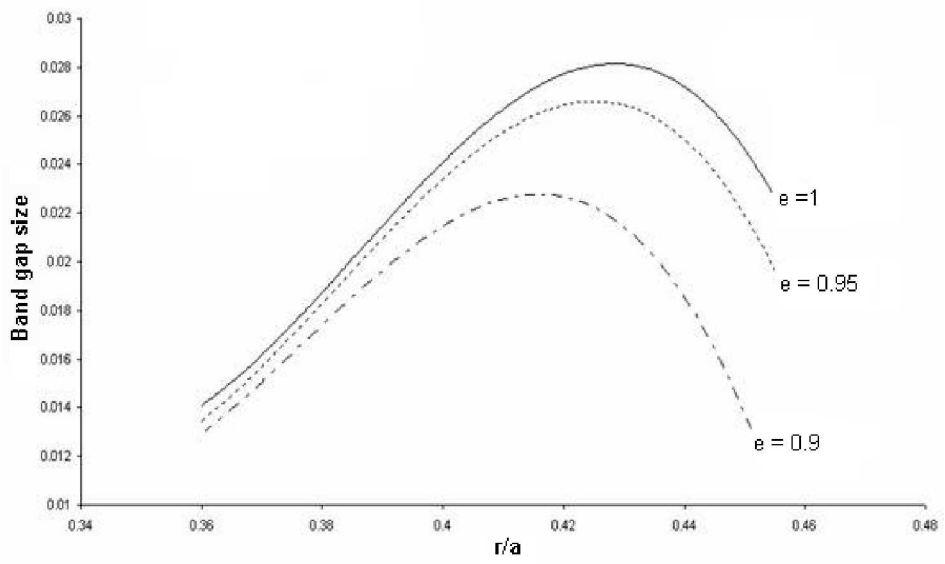

Figure 2. Variation of TE1-2 photonic band gap for PhC structure consisting of square lattice of elliptical air holes in Si with normalized air hole radius 'r/a' keeping the fill factor constant.

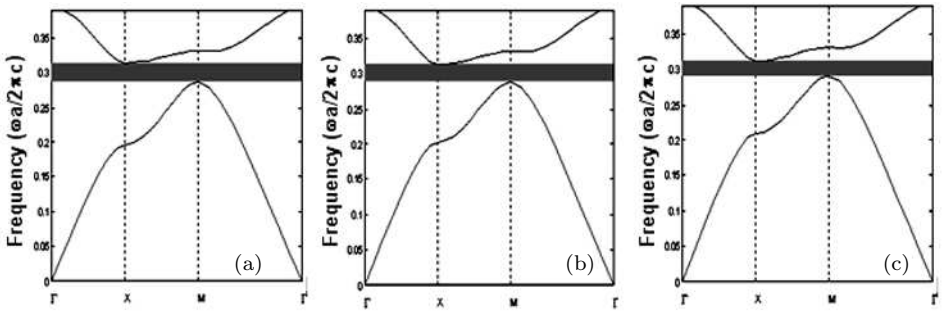

Figure 3. TE1-2 photonic band gap variation for (**a**) $e = 1$, (**b**) $e = 0.95$ and (**c**) $e = 0.9$ for normalized fictive radius of elliptic air holes $r/a = 0.43$ in Si.

Figure 5 shows that the TE1-2 photonic band gaps exhibit an oscillatory behaviour in terms of gap sizes with the variation in the orientation angle of the constituent air holes for $e = 0.95$ and 0.9. The TE band gaps show 90° oscillations. However, the variation becomes more pronounced with increasing ellipticity.

3.2 *PhC composed of square lattice of Si rods in air*

Similar analysis has been done for the second structure, i.e. the PhC composed of Si rods in air as shown in figure 1b using the PWE method.

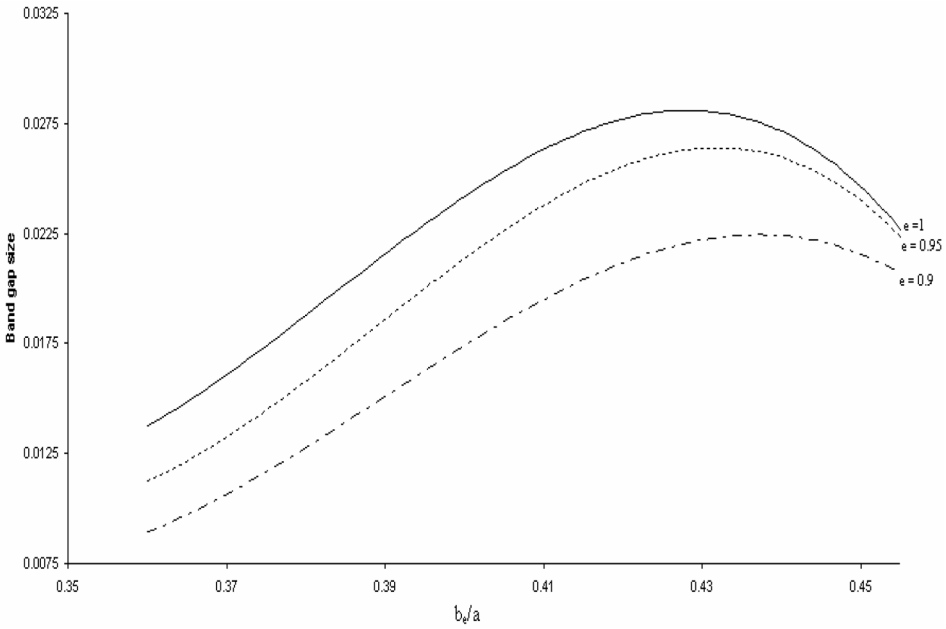

Figure 4. Variation of TE1-2 photonic band gap for a PhC crystal consisting of square lattice of elliptical air holes in Si with normalized major axis b_e/a keeping b_e constant.

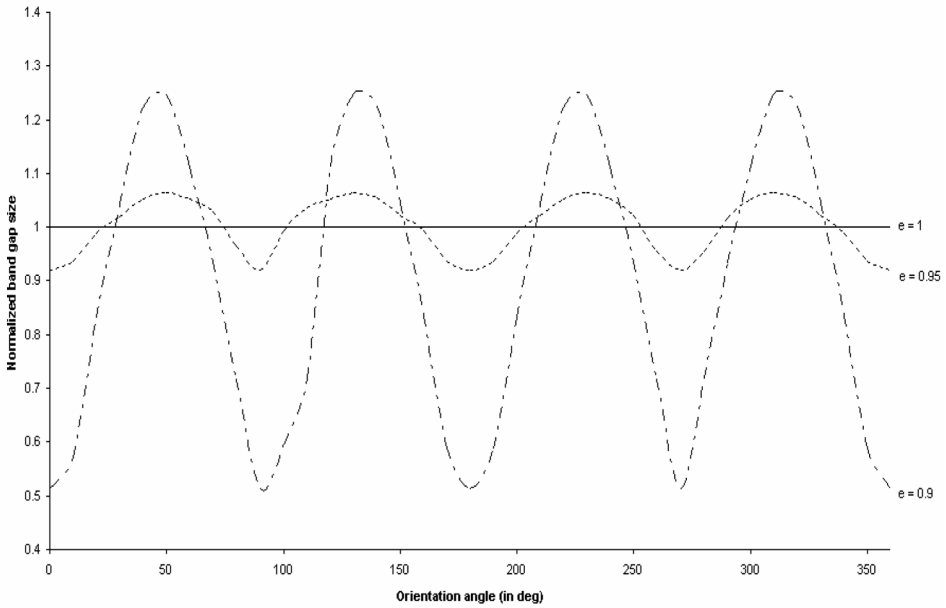

Figure 5. Variation of TE1-2 photonic band gap with the orientation angle of the constituent air holes of the PhC composed of square lattice of air holes in Si for $r/a = 0.43$.

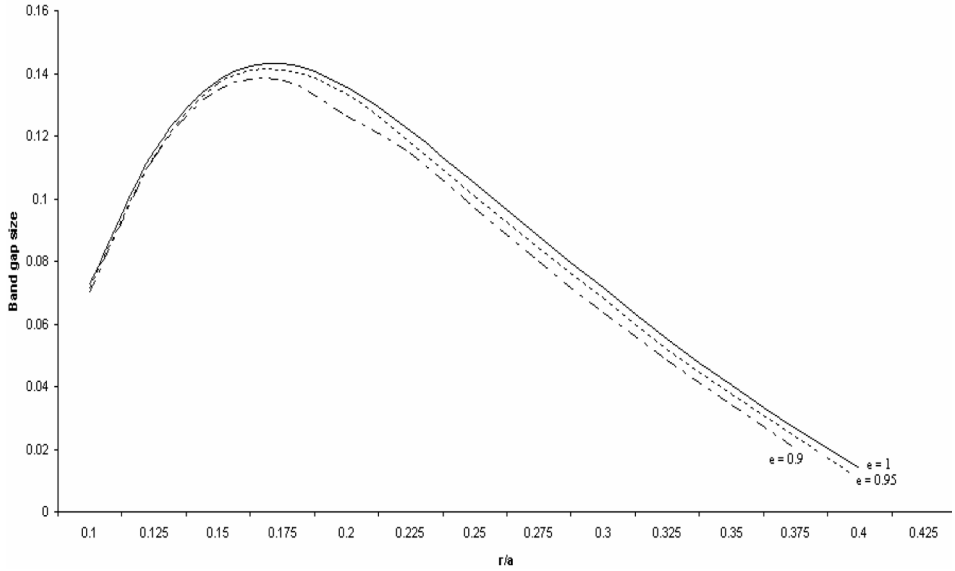

Figure 6. Variation of TM1-2 band gap for a PhC crystal structure composed of square lattice of elliptical Si rods in air with normalized rod radius r/a keeping the fill factor constant.

Figure 6 shows the variation of the TM1-2 photonic band gap size with normalized fictive radius r/a of the constituent Si rods for three different values of ellipticities with constant fill factor. In this case only TM1-2 gap has been studied, as TE1-2 gap does not exist. Figure 7 shows the variation of photonic band gap size with the normalized major axis b_e/a for three different values of ellipticities, i.e. $e = 1$, 0.95 and 0.9, where major axis is kept constant and the ellipticity is induced by changing the minor axis.

In this case only TM1-2 gap has been studied, as TE1-2 gap does not exist. However, similar qualitative behaviour for TM1-2 band gap sizes was observed as was observed for the TE1-2 gap size in the photonic crystal consisting of square lattice of air holes in silicon.

In figures 6 and 7, the photonic band gap size for the TM mode first increases with increasing r/a, becomes maximum and then decreases for all three cases. Figure 8 shows the variation due to change in the orientation angle for normalized rod radius $r/a = 0.25$ for $e = 1$, 0.95 and 0.9.

The TM1-2 photonic band gap size shows an oscillatory behaviour for $e = 0.95$ and 0.9 with a period of 180°.

4. Discussion

The variation in photonic band gap sizes in figures 4 and 7 for the two structures is the combined effect of ellipticity and changing fill factor whereas, the variation of PBG sizes in figures 2 and 6 show the effect of ellipticity as the fill factor is kept

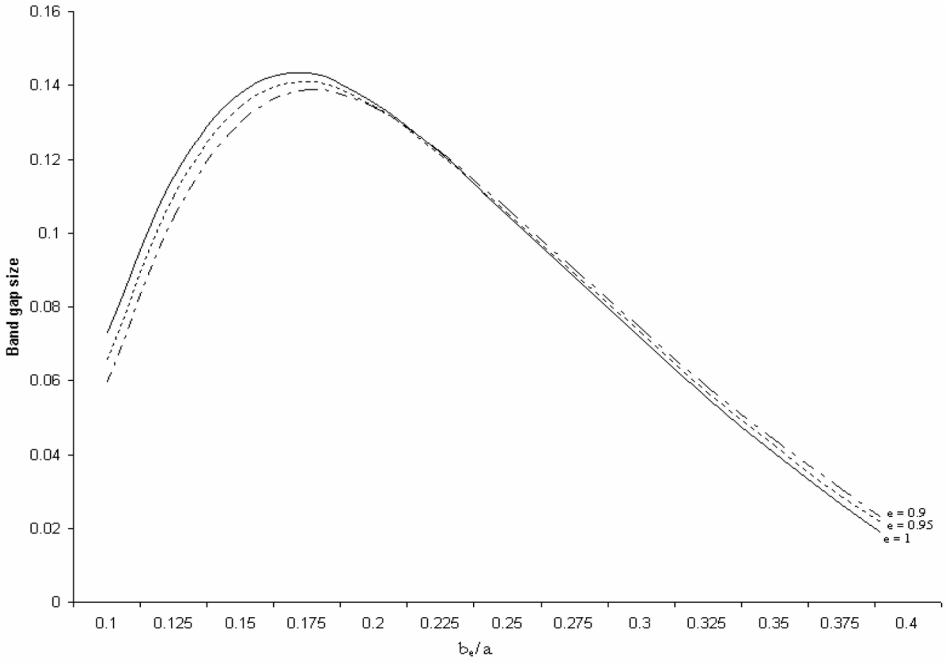

Figure 7. Variation of TM1-2 band gap for a PhC composed of square lattice of elliptical Si rods in air with normalized major axis b_e/a keeping b_e constant.

constant. The variation in photonic band gap sizes due to the orientation angle for the two structures show an oscillatory behaviour of band gap sizes in the two structures as shown in figures 5 and 8.

As a rule of thumb in photonic crystals, TE modes have advantage in photonic crystal structures composed of air holes in dielectric whereas TM modes are favoured in PhC structures composed of dielectric columns in air. It is observed that the photonic band gap size for TE polarization in PhC composed of square lattice of air holes in Si and photonic band gap size for TM polarization in the PhC consisting of Si rods in air show oscillatory behaviour with the change in the orientation angle. It is observed from figure 5 that TE1-2 photonic band gap size shows 90° oscillations with the change in orientation angle of constituent elliptical air holes in dielectric whereas TM1-2 photonic band gap size show an oscillation of 180° with the change in the orientation angle of the constituent elliptical dielectric rods in air. This can be explained by the symmetry considerations.

From the above analysis, we conclude that the photonic band gap along with its polarization sensitivity also depend on the ellipticity of the constituent air holes/dielectric rods in dielectric/air and the orientation angle of the elliptical air holes/dielectric rods. The photonic band gap analysis with the variation in ellipticity can prove helpful in the design of the photonic band gap-based devices.

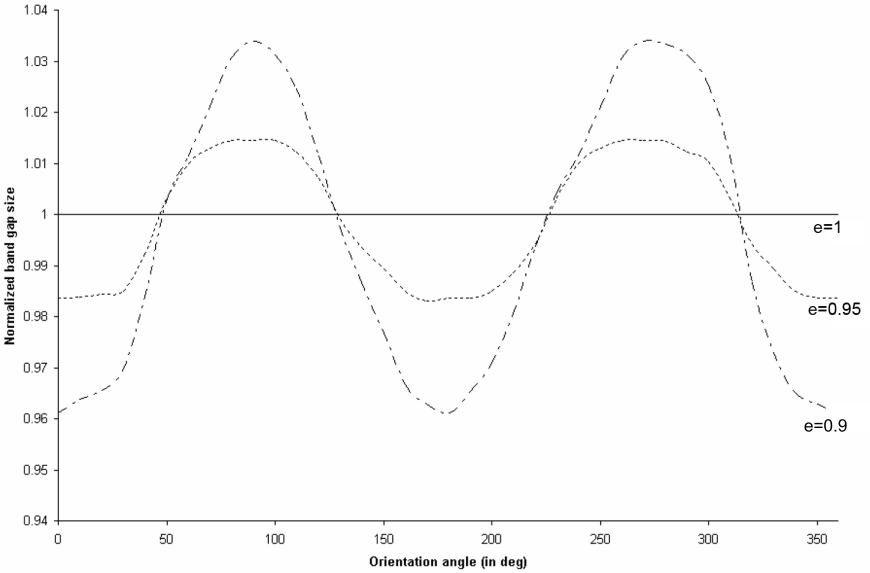

Figure 8. Variation of TM1-2 photonic band gap size with the orientation angle of the constituent Si rods of the PhC composed of square lattice of Si rods in air for $r/a = 0.25$.

Acknowledgement

The authors gratefully acknowledge the financial support provided by All India Council of Technical Education, Government of India for the R&D project 'Propagation Characteristics of Photonic Crystal Fibers and Waveguides for Telecom and Sensing Applications' and initiatives towards establishment of 'TIFAC-Center of Relevance and Excellence in Fiber Optics and Optical Communications at Delhi College of Engineering, Delhi' through 'Mission REACH' program of Technology Vision-2020, Government of India.

References

[1] J D Joannapolous, R D Meade and J N Winn, *Photonic crystals: Molding the flow of light* (Princeton University Press, New Jersey 08540, 1995)
[2] K Sakoda, *Optical properties of photonic crystals* (Springer, Berlin, 2001)
[3] Z Li, J Wang and B Y Gu, *Phys. Rev.* **B58**, 3721 (1998)
[4] D Cassagne, C Jouanin and D Bertho, *Phys. Rev.* **B53**, 7134 (1995)
[5] Z Li, B Y Gu and G Z Yang, *Phys. Rev.* **B81**, 2574 (1998)
[6] R Hillerbrand, W Hergert and W Harms, *Mater. Sci. Semiconductor Processing* **3**, 493 (2000)
[7] R Hillebrand and W Hergret, *Solid State Commun.* **115**, 227 (2000)
[8] M Qiu and S He, *Phys. Rev.* **B60**, 10610 (2000)
[9] C Chen, A Sharkway, D Shi and D W Prather, *Optics Express* **11**, 317 (2003)
[10] Y Kalra and R K Sinha, *Opt. Quantum Electron.* **37**, 889 (2005)
[11] S G Johnson and J D Joannopolous, *Optics Express* **8**, 173 (2001)